Floquet Realization and Signatures of One-Dimensional Anyons in an Optical Lattice

Christoph Sträter,[1] Shashi C. L. Srivastava,[1,2] and André Eckardt[1,*]
[1]Max-Planck-Institut für Physik komplexer Systeme, Nöthnitzer Straße 38, 01187 Dresden, Germany
[2]Variable Energy Cyclotron Centre, 1/AF Bidhan nagar, Kolkata 700 064, India
(Received 26 February 2016; published 10 November 2016)

We propose a simple scheme for mimicking the physics of one-dimensional anyons in an optical-lattice experiment. It relies on a bosonic representation of the anyonic Hubbard model to be realized via lattice-shaking-induced resonant tunneling against potential offsets, which are created by a combination of a lattice tilt and strong on-site interactions. No lasers additional to those used for the creation of the optical lattice are required. We also discuss experimental signatures of the continuous interpolation between bosons and fermions when the statistical angle θ is varied from 0 to π. Whereas the real-space density of the bosonic atoms corresponds directly to that of the simulated anyonic model, this is not the case for the momentum distribution. Therefore, we propose to use Friedel oscillations in the density as a probe for continuous fermionization of the bosonic atoms.

DOI: 10.1103/PhysRevLett.117.205303

Fundamental particles in nature are either bosons or fermions. Bosons obey Bose-Einstein statistics such that their joint wave function is symmetric with respect to the exchange of two particles, whereas fermions obey Fermi-Dirac statistics and the wave function picks up a minus sign under particle exchange. In two dimensions, also anyons would be possible fundamental particles. They obey a fractional statistics that interpolates between bosonic and fermionic behavior [1–5]. If two anyons exchange their position, the wave function pics up a phase. Practically, anyons play a major role as quasiparticles of topologically ordered states of matter such as fractional-quantum-Hall states [6–8], with potential applications in robust topological quantum information processing [9–16]. As shown by Haldane, for quasiparticles the concept of fractional statistics can be extended to arbitrary dimensions [17]. One-dimensional (1D) anyons have recently attracted an increased attention [18–33], including two proposals for their implementation with bosonic atoms in an optical lattice [34,35]. These proposals are based on mapping the anyons via a generalized Jordan-Wigner transformation to bosons with a density-dependent tunneling parameter to be engineered by laser dressing of internal atomic degrees of freedom. However, an experimental realization has not yet been achieved.

In the following, we propose a simple alternative scheme for the experimental realization of 1D anyons, based on time-periodic forcing. It is feasible in existing experimental setups and, in contrast to earlier proposals, does neither rely on the internal atomic structure nor require any lasers additional to those creating the optical lattice. Our scheme is based on engineering an occupation-dependent Peierls phase of the tunneling matrix elements by means of coherent lattice-shaking-assisted tunneling against potential offsets created by a combination of a static potential tilt and strong on-site interactions. The scheme, which is applicable in the low-density regime, also permits us to effectively tune the interactions between the anyons. The fact that periodic forcing has recently been employed already experimentally for engineering both number-dependent tunneling amplitudes [36,37] and non-number-dependent Peierls phases [38–47] (see also Ref. [48] for an overview of Floquet engineering in optical lattices) indicates that the proposed creation of number-dependent Peierls phases by such means is feasible.

We, moreover, discuss experimental signatures of the anyonic model in its ground state using exact diagonalization. Considering small chains, as they can be realized in quantum-gas microscopes [49,50], we monitor experimentally measurable observables that directly reflect anyonic properties and are invariant under the Jordan-Wigner transformation from anyons to bosons. This excludes the momentum distribution, which is altered by the transformation so that the measurable bosonic momentum distribution does not correspond to that of the anyons. It includes, however, on-site densities and their correlations, as well as the second Rényi entropy of the subsystem given by the first ℓ sites. We show that in small systems Friedel oscillations can serve as a signature for the continuous fermionization occurring when the statistical angle θ is varied from 0 to π.

The Hubbard model of one-dimensional lattice anyons with on-site interactions [34] takes the form

$$\hat{H} = -J\sum_{j=2}^{M}(\hat{a}_j^\dagger \hat{a}_{j-1} + \text{H.c.}) + U\sum_{j=1}^{M}\hat{n}_j(\hat{n}_j - 1). \quad (1)$$

Here, the annihilation and creation operators, $\hat{a}_j$ and $\hat{a}_j^\dagger$, for anyons at site j obey the commutation relations $\hat{a}_j\hat{a}_k^\dagger - e^{-i\theta\,\mathrm{sgn}(j-k)}\hat{a}_k^\dagger\hat{a}_j = \delta_{jk}$ and $\hat{a}_j\hat{a}_k - e^{-i\theta\,\mathrm{sgn}(j-k)}\hat{a}_k\hat{a}_j = 0$,

which are parametrized by the statistical angle θ. Here $\mathrm{sgn}(k) = -1, 0, 1$ for $k < 0, = 0, > 0$, respectively, so that on-site the particles behave like bosons. Thus, even for $\theta = \pi$, these lattice anyons are just pseudofermions, since many of them are allowed to occupy the same site. Following Refs. [23,34], the anyonic model can be mapped to the bosonic model

$$\hat{H} = -J\sum_{j=2}^{M}(\hat{b}_j^\dagger \hat{b}_{j-1} e^{i\theta\hat{n}_j} + \text{H.c.}) + U\sum_{j=1}^{M}\hat{n}_j(\hat{n}_j - 1), \quad (2)$$

via the generalized Jordan-Wigner transformation $\hat{a}_j = \hat{b}_j \exp(i\theta\sum_{k=j+1}^{M}\hat{b}_k^\dagger\hat{b}_k)$. Here the anyonic exchange phase has been translated to a density-dependent Peierls phase: when tunneling one site to the right (left), a boson pics up a phase given by θ ($-\theta$) times the number of particles occupying the site it jumps to (from). Thus, if two particles pass each other via two subsequent tunneling processes to the right (left), the many-body wave function pics up a phase of θ ($-\theta$). These tunneling processes are illustrated in Fig. 1(a).

For the realization of the number-dependent tunneling phase, we consider bosons in a tilted periodically forced lattice described by the Hamiltonian

$$\hat{H}(t) = \sum_j \Big(-J'[\hat{b}_j^\dagger\hat{b}_{j-1} + \text{H.c.}] + \frac{U'}{2}\hat{n}_j(\hat{n}_j - 1) + V_j\hat{n}_j + [\Delta + F(t)]j\hat{n}_j\Big). \quad (3)$$

Here, $J' > 0$ and $U' > 0$ denote the bare tunneling and interaction parameters, $\Delta > 0$ characterizes a strong potential tilt, V_j captures possible weak additional on-site potentials, and $F(t) = F(t+T)$ incorporates a homogeneous time-periodic force of angular frequency $\omega = 2\pi/T$ with vanishing cycle average $1/T\int_0^T dtF(t) = 0$. It can be implemented as an inertial force $F(t)/a = -m\ddot{x}(t)$, with lattice constant a, by shaking the lattice position $x(t)$ back and forth. We require the resonance conditions

$$\Delta = \hbar\omega, \qquad U' = 2\hbar\omega + U, \quad (4)$$

as well as the high-frequency conditions

$$J', |U|, |V_j - V_{j-1}| \ll \hbar\omega, \quad (5)$$

where we have introduced the small interaction detuning U. The largest share of the on-site energy is then given by $\hat{H}_0 = \hbar\omega\sum_j[\hat{n}_j(\hat{n}_j - 1) + j\hat{n}_j]$, so that tunneling is energetically suppressed. Namely, when a particle tunnels from $j-1$ to j this energy changes by $\hbar\omega\hat{\nu}_{j,j-1}$ with $\hat{\nu}_{j,j-1} = 2(\hat{n}_j - \hat{n}_{j-1}) + 3 = \pm\hbar\omega, \pm 3\hbar\omega, \ldots$. However, coherent tunneling processes can be induced by time-periodic forcing as ν-"photon" processes, where the drive provides or absorbs $|\nu|$ energy quanta $\hbar\omega$. They are described by an effective tunneling matrix element [51,52], which, through $\hat{\nu}_{j,j-1}$, will depend on the occupation numbers. Such number-dependent resonant tunneling has recently been investigated both experimentally [36] and theoretically [53,54] (see also Ref. [55]). As we will show now, it can be used to achieve the number-dependent tunneling phases appearing in Eq. (2).

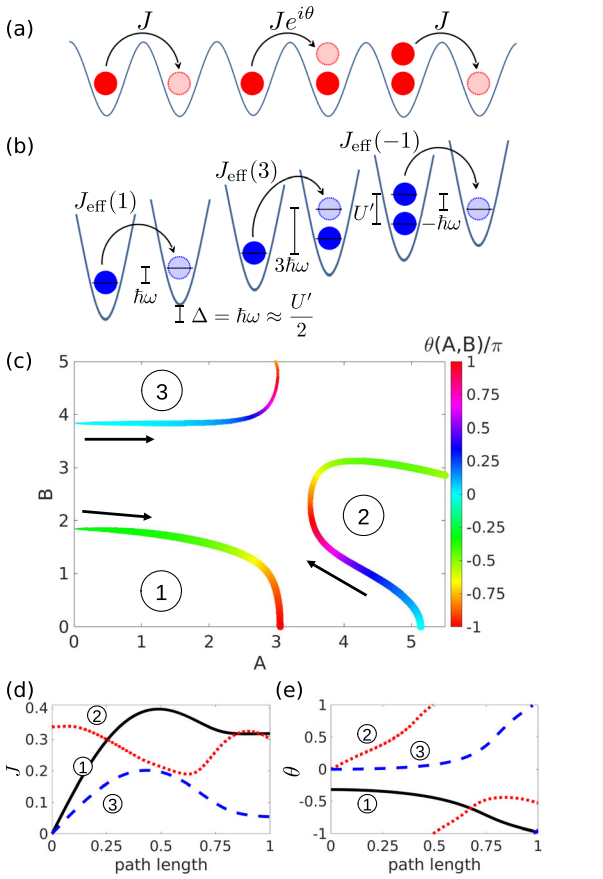

FIG. 1. (a) Basic number-dependent tunneling processes involving up to two bosons. We only depict rightwards tunneling, the leftwards processes are Hermitian conjugated. (b) Realization as 1, 3, and -1 photon processes in a tilted lattice with strong on-site interactions U' (b). We depict processes for tunneling rightwards; tunneling leftwards is simply described by conjugated processes. (c) Parameter curves that fulfill $|J_{\text{eff}}(1)| = |J_{\text{eff}}(3)|$. The color of the lines represents the statistical angle $\theta = \arg[J_{\text{eff}}(3)/J_{\text{eff}}(1)]$ and their thickness the tunneling amplitude $J = |J_{\text{eff}}(1)|$. (d),(e) θ and J following the lines in (b) in the direction of the arrow.

Using the time-periodic unitary operator

$$\hat{U}(t) = \exp\Big(-i\sum_j[\omega t\hat{n}_j(\hat{n}_j - 1) + \{\omega t - \chi(t)\}j\hat{n}_j]\Big), \quad (6)$$

where $\chi(t) = (am/\hbar)\dot{x}(t)$ so that $\hbar\dot{\chi}(t) = -F(t)$, we can perform a number-dependent gauge transformation. It integrates out the strong on-site terms $\hat{H}_0$ as well as the periodic force, but leads to number-dependent tunneling terms $-J'\hat{b}_j^\dagger\hat{b}_{j-1}\exp[i\omega t\hat{\nu}_{j,j-1} - i\chi(t)]$ in the

new Hamiltonian $\hat{U}^\dagger(t)\hat{H}(t)\hat{U}(t) - i\hbar\hat{U}^\dagger(t)\partial_t\hat{U}(t)$. Averaging over the rapidly oscillating phase factor by integrating over one driving period (corresponding to the leading order of a high-frequency approximation [61–63]), we obtain the effective time-independent Hamiltonian

$$\hat{H}_{\mathrm{eff}} = -\sum_j (\hat{b}_j^\dagger \hat{b}_{j-1} J_{\mathrm{eff}}(\hat{\nu}_{j,j-1}) + \mathrm{H.c.}) + \sum_j \left(\frac{U}{2}\hat{n}_j(\hat{n}_j - 1) + V_j\hat{n}_j\right). \quad (7)$$

It contains the number-dependent tunneling parameter

$$J_{\mathrm{eff}}(\nu) = \frac{J'}{T}\int_0^T dt \exp\left(i\omega t\nu - i\chi(t)\right), \quad (8)$$

and the tunable interaction parameter $U = U' - 2\hbar\omega$, which can take both negative and positive values.

The effective tunneling matrix elements $J_{\mathrm{eff}}(\nu)$ should reproduce the number-dependent tunneling parameters of Eq. (2). We restrict ourselves to the low-density regime, where the dominant processes involve one or two bosons. These processes are those depicted in Fig. 1(a) as well as the Hermitian conjugated processes for tunneling leftwards. As illustrated in Fig. 1(b), these processes are associated with different potential energy changes $\nu\hbar\omega$. Tunneling rightwards from a singly or doubly occupied site onto an empty site corresponds to $\nu = 1$ or $\nu = -1$, respectively, and should be described by the parameter,

$$J_{\mathrm{eff}}(1) = J_{\mathrm{eff}}(-1) = Je^{i\phi_g}, \quad (9)$$

with real tunneling amplitude J and arbitrary Peierls phase ϕ_g reflecting the freedom of gauge. Tunneling rightwards from an empty site onto an occupied site is associated with $\nu = 3$ and the corresponding tunneling parameter should carry an additional phase θ,

$$J_{\mathrm{eff}}(3) = Je^{i\theta + i\phi_g}. \quad (10)$$

In order to fulfill conditions (9) and (10), we make the simple ansatz

$$\chi(t) = A\cos(\omega t) + B\cos(2\omega t) \quad (11)$$

for the (integrated) driving force (other choices are possible). This ansatz already ensures that $J_{\mathrm{eff}}(1) = J_{\mathrm{eff}}(-1)$. The additional constraint $|\mathrm{J}_{\mathrm{eff}}(3)| = J = |J_{\mathrm{eff}}(1)|$ defines lines in the $A - B$ plane, as can be seen in panel (c) of Fig. 1. The thickness and the color of the plotted lines represents the tunneling amplitude J and the statistical angle θ, respectively. The variation of J and θ along the lines is also plotted in panels (d) and (e). Whereas lines 2 and 3 cover the full range $|\theta| \in [0, \pi]$, line 1 roughly allows us to realize $|\theta| \in [0.4\pi, \pi]$.

A clear signature of the continuous fermionization of the system with increasing θ is the formation of a Fermi sea in the momentum distribution of the anyons (see, e.g., Ref. [32]). However, in an experiment one cannot measure the anyonic momentum distribution, but only the bosonic one, which, due to both the Jordan-Wigner transformation and the gauge transformation (6) differs from that of the anyons. Therefore, in the following we will consider only such observables that are invariant under these transformations. These include the densities $n_i = \langle\hat{n}_i\rangle$, the two-particle correlations $\chi_{i,j} = \langle b_i^\dagger b_j^\dagger b_j b_i\rangle/(n_i n_j)$, and also the second Rényi entropy characterizing the purity of the reduced density matrix $\hat{\rho}_\ell$ of the subsystem given by the first ℓ sites $j = 1, \ldots, \ell$, $S_\ell = -\ln \mathrm{Tr}(\hat{\rho}_\ell^2)$ [64]. In the following, we will focus on ground-state properties, so that S_ℓ is an entanglement entropy (as it has been measured recently in a bosonic chain [49]).

We compute n_i, $\chi_{i,j}$, and S_ℓ using exact diagonalization both for the ideal model (2) and the effective Hamiltonian (7). We consider $N = 4$ bosons on $M = 20$ sites, corresponding to a density of $n = 0.2$. The effective tunneling matrix elements (8) were obtained for the driving function corresponding either to path 1 of Fig. 1(c) or to path 2, in case the desired statistical angle $|\theta|$ is not available in path 1. Despite the fact that they reproduce the ideal tunneling matrix elements only for processes involving one and two particles, we find very good agreement between the ideal and the effective model: In Figs. 2(a) and 2(b), we plot n_i and S_ℓ for the effective model with $U = 0$ and various anyonic angles θ. The results match very well with those obtained for the ideal model shown in Figs. 2(c) and 2(d). For nonzero on-site interactions, $U/J \equiv \tan(\phi/2)$ the agreement is equally good, so that we only plot the results for the ideal model in Figs. 2(e) and 2(f).

In Fig. 2(c), we can observe that the density distribution flattens in the center, when the statistical angle is switched on. This effect can be understood by noting that the scattering properties resulting from the density dependent tunneling resemble those of repulsive on-site interactions [35], which favor a flat density. For large θ, the density becomes modulated, with one maximum for each particle in the system. These oscillations correspond to Friedel oscillations, which are a hallmark of fermionic behavior [65]. They are a finite-size effect induced by the hard-wall boundary conditions (as they can be realized in quantum-gas microscopes). Their wavelength is roughly given by π/k_F, with Fermi wave number k_F, corresponding to the average particle distance, which in our system is given by $n^{-1} = 5$ lattice constants. Generally, Friedel oscillations occur in the vicinity of localized defects. Their buildup allows us to monitor the continuous fermionization of the 1D anyons in a system of bosons with number-dependent tunneling. The oscillations are also clearly visible in the entanglement entropy [Fig. 2(d)]. An intuitive explanation is that the maximum corresponds to the position of a particle, whose delocalization within the maximum contributes to the entanglement between the left and right subsystems.

In Figs. 2(e), 2(f), showing data for a system with significant on-site interactions $U/J = \tan(\pi/4) = 1$, the fermionic signatures occur already for smaller θ.

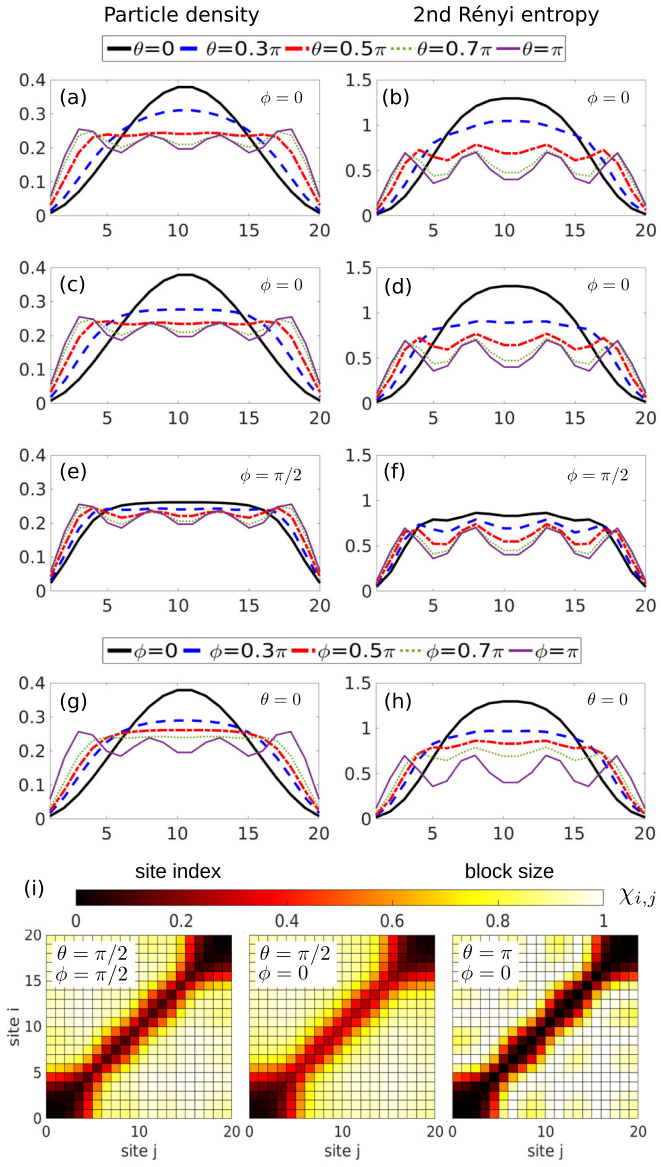

FIG. 2. Ground-state properties: Density n_i and entanglement entropy S_ℓ of the first ℓ sites. Either the anyonic angle θ is varied (a)–(f) or the relative interaction strength $U/J = \tan(\phi/2)$ (g),(h). Computed for the effective Hamiltonian (7) (a),(b), the ideal model (2) (c)–(f), and plain bosons (g),(h). (i) Two-particle correlations function $\chi_{i,j} = \langle b_i^\dagger b_j^\dagger b_j b_i \rangle / (n_i n_j)$ for various anyonic angles θ and interaction strengths $U/J = \tan(\phi/2)$ for the effective Hamiltonian (7).

This observation is consistent with the well-known fact that increasing the on-site interactions is another way of approaching fermionic behavior [66]. This is illustrated also in Figs. 2(g), 2(h) showing data for plain bosons ($\theta = 0$) and different U/J. In the hard-core limit ($\phi = \pi$), the bosons can be mapped to fermions. Despite the fact that 1D anyons only become pseudofermions for $\theta = \pi$, the data for $\theta = \pi$ in Figs. 2(c), 2(d) agree very well with those for $\phi = \pi$ in Figs. 2(g), 2(h). This suggests that for low densities pseudofermions behave like true fermions.

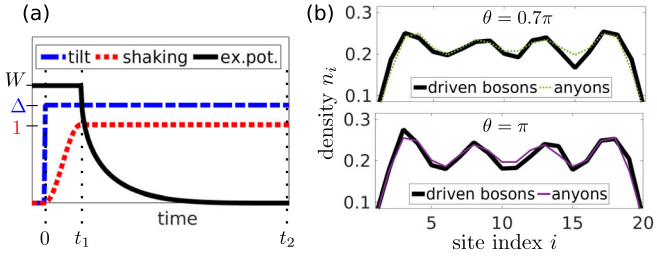

FIG. 3. State preparation for a system of 4 particles on 20 sites, simulated using the full time-dependent Hamiltonian (3). (a) Preparational protocol. (b) Density distribution of the final state compared to the ground state of the anyon model (1). We have chosen realistic parameters for an optical lattice of depth $V_0 = 10E_R$ giving $J' = 0.0192E_R$, where the recoil energy E_R typically corresponds to frequencies of a few kHz [67]. Moreover, we chose $\hbar\omega = E_R - U$ (well below the band gap of $\approx 5E_R$), $U = 0.5J$, $W = 0.6E_R$, $t_1 = 50T$, and $t_2 = 1240T(1300T) \approx 50\hbar/J$ for $\theta = 0.7\pi(\pi)$.

This is confirmed also by the correlations shown in Fig. 2(i). Their diagonal elements $\chi_{j,j} = \langle \hat{n}_j(\hat{n}_j - 1) \rangle / n_j^2$, which are a measure for double occupation, vanish for $\theta = \pi$, even though pseudofermions locally behave like bosons. Simulations show that pseudofermions behave like fermions up to a filling of about one-third [54]. This is also the filling where the low-density description, stating that driven bosons behave like anyons, is found to break down [54].

The buildup of Friedel oscillations requires the system to be quantum degenerate, i.e., temperatures $\mathcal{T}$ well below the Fermi energy $E_F = 2J[1 - \cos(k_F)] \approx J\pi^2 n^2$, so that the thermal wavelength is large compared to the mean particle distance. Computing canonical expectation values for $N = 4$ anyons on $M = 20$ sites for the finite temperature $\mathcal{T}/J = 0.1$ (corresponding to a von Neumann entropy per particle of $s \approx 0.20$, which is accessible in a system of spinless bosons), we find well-pronounced Friedel oscillations [54]. In an experiment, the low-entropy state of the effective Hamiltonian (7) has to be prepared starting from a low-entropy state of the undriven system. Let us assume that initially $\Delta = F = 0$ and the system is prepared in a Mott-insulator state $|S\rangle = \prod_{j \in S} \hat{b}_j^\dagger |\text{vac}\rangle$, with the set S containing N lattice sites and $|\text{vac}\rangle$ denoting the vacuum state. This is the asymptotic ground state in the presence of an external potential $V_j = -W\delta_{j \in S}$ in the limit W, $U' \gg J$. For finite U, this is also the ground state of the effective model (7), with $J_{\text{eff}}(\nu) = 0$. Thus, we can adiabatically melt the Mott insulator into the ground state of $\hat{H}_{\text{eff}}$ by smoothly ramping up the forcing, i.e., the $J_{\text{eff}}(\nu)$, and then continuously switching off the external potential W. In order to minimize the mass transport during this adiabatic process, it is useful that S contains equally spaced lattice sites, so that V_i describes a superlattice. We have simulated this protocol integrating the time evolution of

the full time-dependent Hamiltonian (3) and find excellent agreement between the final state and the ground state of H_{eff} [Fig. 3]. This confirms both a description in terms of the effective Hamiltonian and the proposed preparation scheme.

In summary, we proposed a simple scheme for the realization of 1D anyons, which is feasible in existing experimental setups. It is based on Floquet engineering a system of bosonic atoms with number-dependent tunneling phases. We, moreover, showed that Friedel oscillations can serve as a directly measurable signature for the continuous fermionization of the anyons.

We thank Sebastian Greschner, Axel Pelster, and Luis Santos for useful discussions. C. S. is grateful for support by the Studienstiftung des deutschen Volkes. This work was supported by the DFG via the Research Unit (Forschergruppe) FOR 2414.

*eckardt@pks.mpg.de

[1] J. M. Leinaas and J. Myrheim, Nuovo Cimento Soc. Ital. Fis. **37**, 1 (1977).
[2] G. A. Goldin, R. Menikoff, and D. H. Sharp, J. Math. Phys. (N.Y.) **22**, 1664 (1981).
[3] F. Wilczek, Phys. Rev. Lett. **49**, 957 (1982).
[4] D. C. Tsui, H. L. Stormer, and A. C. Gossard, Phys. Rev. Lett. **48**, 1559 (1982).
[5] G. S. Canright, S. M. Girvin, and A. Brass, Phys. Rev. Lett. **63**, 2291 (1989).
[6] R. B. Laughlin, Phys. Rev. Lett. **50**, 1395 (1983).
[7] B. I. Halperin, Phys. Rev. Lett. **52**, 1583 (1984).
[8] F. E. Camino, W. Zhou, and V. J. Goldman, Phys. Rev. B **72**, 075342 (2005).
[9] A. Kitaev, Ann. Phys. (Amsterdam) **303**, 2 (2003).
[10] S. D. Sarma, M. Freedman, and C. Nayak, Phys. Rev. Lett. **94**, 166802 (2005).
[11] P. Bonderson, A. Kitaev, and K. Shtengel, Phys. Rev. Lett. **96**, 016803 (2006).
[12] A. Stern and B. I. Halperin, Phys. Rev. Lett. **96**, 016802 (2006).
[13] C. Nayak, S. H. Simon, A. Stern, M. Freedman, and S. D. Sarma, Rev. Mod. Phys. **80**, 1083 (2008).
[14] J. Alicea, Y. Oreg, G. Refael, F. von Oppen, and M. P. Fisher, Nat. Phys. **7**, 412 (2011).
[15] A. Stern and N. H. Lindner, Science **339**, 1179 (2013).
[16] J. C. Matthews, K. Poulios, J. D. Meinecke, A. Politi, A. Peruzzo, N. Ismail, K. Wörhoff, M. G. Thompson, and J. L. O'Brien, Sci. Rep. **3**, 1539 (2013).
[17] F. D. M. Haldane, Phys. Rev. Lett. **67**, 937 (1991).
[18] Z. N. C. Ha, Phys. Rev. Lett. **73**, 1574 (1994).
[19] M. V. N. Murthy and R. Shankar, Phys. Rev. Lett. **73**, 3331 (1994).
[20] Y.-S. Wu and Y. Yu, Phys. Rev. Lett. **75**, 890 (1995).
[21] J.-X. Zhu and Z. D. Wang, Phys. Rev. A **53**, 600 (1996).
[22] L. Amico, A. Osterloh, and U. Eckern, Phys. Rev. B **58**, R1703 (1998).
[23] A. Kundu, Phys. Rev. Lett. **83**, 1275 (1999).
[24] M. T. Batchelor, X.-W. Guan, and N. Oelkers, Phys. Rev. Lett. **96**, 210402 (2006).
[25] M. D. Girardeau, Phys. Rev. Lett. **97**, 100402 (2006).
[26] P. Calabrese and M. Mintchev, Phys. Rev. B **75**, 233104 (2007).
[27] A. del Campo, Phys. Rev. A **78**, 045602 (2008).
[28] Y. Hao, Y. Zhang, and S. Chen, Phys. Rev. A **78**, 023631 (2008).
[29] Y. Hao, Y. Zhang, and S. Chen, Phys. Rev. A **79**, 043633 (2009).
[30] Y. Hao and S. Chen, Phys. Rev. A **86**, 043631 (2012).
[31] L. Wang, L. Wang, and Y. Zhang, Phys. Rev. A **90**, 063618 (2014).
[32] G. Tang, S. Eggert, and A. Pelster, New J. Phys. **17**, 123016 (2015).
[33] W. Zhang, E. Fan, T. C. Scott, and Y. Zhang, arXiv:1511.01712.
[34] T. Keilmann, S. Lanzmich, I. McCulloch, and M. Roncaglia, Nat. Commun. **2**, 361 (2011).
[35] S. Greschner and L. Santos, Phys. Rev. Lett. **115**, 053002 (2015).
[36] R. Ma, M. E. Tai, P. M. Preiss, W. S. Bakr, J. Simon, and M. Greiner, Phys. Rev. Lett. **107**, 095301 (2011).
[37] F. Meinert, M. J. Mark, K. Lauber, A. J. Daley, and H.-C. Nägerl, Phys. Rev. Lett. **116**, 205301 (2016).
[38] M. Aidelsburger, M. Atala, S. Nascimbène, S. Trotzky, Y.-A. Chen, and I. Bloch, Phys. Rev. Lett. **107**, 255301 (2011).
[39] J. Struck, C. Ölschläger, R. Le Targat, P. Soltan-Panahi, A. Eckardt, M. Lewenstein, P. Windpassinger, and K. Sengstock, Science **333**, 996 (2011).
[40] J. Struck, C. Ölschläger, M. Weinberg, P. Hauke, J. Simonet, A. Eckardt, M. Lewenstein, K. Sengstock, and P. Windpassinger, Phys. Rev. Lett. **108**, 225304 (2012).
[41] J. Struck, M. Weinberg, C. Ölschläger, P. Windpassinger, J. Simonet, K. Sengstock, R. Höppner, P. Hauke, A. Eckardt, M. Lewenstein, and L. Mathey, Nat. Phys. **9**, 738 (2013).
[42] M. Aidelsburger, M. Atala, M. Lohse, J. T. Barreiro, B. Paredes, and I. Bloch, Phys. Rev. Lett. **111**, 185301 (2013).
[43] H. Miyake, G. A. Siviloglou, C. J. Kennedy, W. C. Burton, and W. Ketterle, Phys. Rev. Lett. **111**, 185302 (2013).
[44] M. Atala, M. Aidelsburger, M. Lohse, J. T. Barreiro, B. Paredes, and I. Bloch, Nat. Phys. **10**, 588 (2014).
[45] G. Jotzu, M. Messer, T. U. Rémi Desbuquois, M. Lebrat, D. Greif, and T. Esslinger, Nature (London) **515**, 237 (2014).
[46] M. Aidelsburger, M. Lohse, C. Schweizer, M. Atala, J. T. Barreiro, S. Nascimbène, N. R. Cooper, I. Bloch, and N. Goldman, Nat. Phys. **11**, 162 (2015).
[47] C. J. Kennedy, W. C. Burton, W. C. Chung, and W. Ketterle, Nat. Phys. **11**, 859 (2015).
[48] A. Eckardt, arXiv:1606.08041.
[49] R. Islam, R. Ma, P. M. Preiss, M. E. Tai, A. Lukin, M. Rispoli, and M. Greiner, Nature (London) **528**, 77 (2015).
[50] T. Fukuhara, S. Hild, J. Zeiher, P. Schauß, I. Bloch, M. Endres, and C. Gross, Phys. Rev. Lett. **115**, 035302 (2015).
[51] A. Eckardt and M. Holthaus, Europhys. Lett. **80**, 50004 (2007).
[52] C. Sias, H. Lignier, Y. P. Singh, A. Zenesini, D. Ciampini, O. Morsch, and E. Arimondo, Phys. Rev. Lett. **100**, 040404 (2008).

[53] A. Bermudez and D. Porras, New J. Phys. **17**, 103021 (2015).
[54] See Supplemental Material at http://link.aps.org/supplemental/10.1103/PhysRevLett.117.205303, which contains an investigation of the role of density and temperature.
[55] An alternative approach for Floquet engineering number-dependent tunneling matrix elements relies on a modulation of the interaction strength [37,56–60].
[56] J. Gong, L. Morales-Molina, and P. Hänggi, Phys. Rev. Lett. **103**, 133002 (2009).
[57] A. Rapp, X. Deng, and L. Santos, Phys. Rev. Lett. **109**, 203005 (2012).
[58] S. Greschner, L. Santos, and D. Poletti, Phys. Rev. Lett. **113**, 183002 (2014).
[59] M. DiLiberto, C. E. Creffield, G. I. Japaridze, and C. Morais Smith, Phys. Rev. A **89**, 013624 (2014).
[60] T. Wang, X.-F. Zhang, F. E. A. dos Santos, S. Eggert, and A. Pelster, Phys. Rev. A **90**, 013633 (2014).
[61] N. Goldman and J. Dalibard, Phys. Rev. X **4**, 031027 (2014).
[62] M. Bukov, L. D'Alessio, and A. Polkovnikov, Adv. Phys. **64**, 139 (2015).
[63] A. Eckardt and E. Anisimovas, New J. Phys. **17**, 093039 (2015).
[64] The Fock states $|\boldsymbol{n}\rangle_c = |n_1\rangle_c|n_2\rangle_c \cdots |n_M\rangle_c$ for 1D anyons ($c = a$) and bosons ($c = b$) obey the Jordan-Wigner transformation $|\boldsymbol{n}\rangle_a = \exp(-i\theta \sum_{j=1}^{M} \sum_{k=j+1}^{M} n_k)|\boldsymbol{n}\rangle_b$. It corresponds to independent site-local transformations $|n_j\rangle_a = \exp(-i\theta(j-1)n_j)|n_j\rangle_b$, so that tracing out a site k is identical for bosons and 1D anyons, $\sum_{n_k a}\langle n_k| \cdot |n_k\rangle_a = \sum_{n_k b}\langle n_k| \cdot |n_k\rangle_b$.
[65] J. Friedel, Nuovo Cimento **7**, 287 (1958).
[66] B. Paredes, A. Widera, V. Murg, O. Mandel, S. Fölling, I. Cirac, G. V. Shlyapnikov, T. W. Hänsch, and I. Bloch, Nature (London) **429**, 277 (2004).
[67] I. Bloch, J. Dalibard, and W. Zwerger, Rev. Mod. Phys. **80**, 885 (2008).